Journal of the Brazilian Society of Mechanical Sciences and Engineering (2020) 42:421
https://doi.org/10.1007/s40430-020-02473-5

TECHNICAL PAPER

# Dynamic characteristics of abrasive grains and machined surface features for variable axis diamond grinding of quartz glass

**Xiaoxiao Chen[1,2] · Heng Wang[1,2] · Wenwu Zhang[1,2]**

Received: 6 February 2020 / Accepted: 22 June 2020 / Published online: 21 July 2020
© The Brazilian Society of Mechanical Sciences and Engineering 2020

**Abstract**
There is a fine application prospect for multi-axis grinding of hard and brittle materials with diamond ball end tool. The effects of tool inclination angles and grinding modes of multi-axis grinding of quartz glass on the dynamic characteristics of the diamond abrasives, surface topography, surface fragmentation phenomenon, and surface roughness were investigated in this work. Material removal characteristics and surface formation conditions would be significantly affected by the effective cutting speed, material stress characteristics, and movement space path derived from different grinding modes and tool inclination angles. The surface texture direction is mainly determined by feed direction of the cutter and initial cutting moment and geometry feature of the engaged diamond abrasives. The surface fragmentation phenomenon of the formed surface is apparent when the corresponding surface roughness values are relatively larger. The machined surface with significant surface fragmentation phenomenon is mainly produced by materials' brittle fracture modes, such as larger positive *lead* and smaller negative *tilt* under conventional grinding and smaller negative *lead* angles and larger positive *tilt* angles under down grinding. Ideal surface evenness could be obtained by using *lead* or *tilt* 0° for conventional and down grinding. The ground surface with smaller surface roughness could be produced when employing tool postures, such as negative *lead* or positive *tilt* under conventional grinding and positive *lead* or negative *tilt* under down grinding condition.

**Keywords** Inclination angles · Surface features · Diamond abrasive · Roughness · Quartz glass

## 1 Introduction

Demands for machining of glass have been increasing in manufacture fields [1, 2]. Quartz glass is a typical hard and brittle material that is difficult to process and has excellent performance in optical instruments, semiconductors, and precision equipment [3, 4]. Multi-axis milling plays a major role in industry technology [5]. Diamond grinding is an effective machining operation for hard and brittle materials [6]. Multi-axis milling with the diamond cutter is an important process technology for processing of hard and brittle materials with complex features, which has broad application prospects.

The machining mechanism, crack, surface roughness, and subsurface damage are hot research issues. The process parameters directly or indirectly affect the surface roughness, crack formation, and subsurface damage. As two objects act directly, workpiece material properties and machining tool features, such as cutting-edge radius, are critical influencing factors for the uncut chip thickness, and the material removal modes are further affected [7]. Ductile machining happened when producing uncut chip thickness under a critical value for brittle materials [8]. The formed surface is directly determined by the process parameters, such as radial depth of cut, and the crack-free surface could be produced by obtaining the critical cutting condition based on the analysis of subsurface damage [9]. Surface roughness is a key evaluation factor of the surface quality and could be predicted by the physics-based model that considers the tool, material properties, and machining parameters [10]. Perveen

Technical Editor: Izabel Fernanda Machado, Dr.

✉ Xiaoxiao Chen
chenxiaoxiao@nimte.ac.cn

✉ Wenwu Zhang
zhangwenwu@nimte.ac.cn

[1] Ningbo Institute of Materials Technology and Engineering, Chinese Academy of Sciences, Ningbo 315201, Zhejiang, China

[2] University of Chinese Academy of Sciences, Beijing 100049, China

et al. [11] focused on the microgrinding of glass materials and analyzed the variations in surface roughness when feed, axial depth of cut, and spindle speed increase. In addition, there is a certain relationship between the surface roughness and the surface damage when grinding BK7 glass, and also the abrasive grain influences the squeezing effect caused by the angle of the abrasive particles which has a certain contribution to the interaction process [12].

Brittle fracture and edge chipping are important phenomena for machining of brittle materials, such as optimal glass. Ductile machining can effectively avoid the adverse effects of material's brittle fracture on the surface quality of the machined surface. Qiu et al. [13] found that cutting thickness, cutter shapes, and spindle speeds significantly affect the machining mechanics in microball end milling of glass. Ab Karim et al. [14] studied the optimal process plans for minimizing edge chipping, and lubrication condition, spindle speed, feed speed, and depth of cut apparently influence the edge chipping for glass milling. Cutting regime in the ductile mode is beneficial to the generation of high-quality surface, and the tool posture and cutting angle are important factors to control the characteristics of cutting. Arif et al. [15] investigated the cutting process and surface generated by ductile-mode machining of silicon, and the inclination angle between the workpiece surface and tool axis was set to improve surface finish. Fracture-free microslots could be processed on silicon wafer when controlling feed rate below a certain value for microball end milling. Hence, tool inclination angle is also a key factor which influences the cutting regime transition in micromachining of brittle materials. A certain tool inclination with a specific feed rate will result in different material removal modes at certain spatial locations in the machining area. Foy et al. [16] investigated the cutting regime transition in microball end milling crown glass by varying tilt angle and feed rate. Material removal modes are closely related to the undeformed chip thickness [8], and crack-free glass surface could be generated in the ductile mode adopting 45° tilt angle and feed speed up to 0.32 mm/min. Guo et al [17] studied the ductile machining under various rake angles based on the SPH simulation model and found that the tool negative rake angle is beneficial to promote the ductile machining of quartz glass. Considering the actual diamond tool processing, the cutting angles of the abrasive grain to remove the processed material will also have an important influence on the mechanical force and material removal modes.

Conventional multi-axis milling of elastic–plastic materials with metal cutting tool is a key technology for metal parts processing [18], and the materials behavior and machining effects for multi-axis diamond grinding of hard and brittle materials also need to be further investigated for extending the application of multi-axis grinding technology in aerospace, medical engineering, optics, and semiconductor fields.

Researches on the influence of cutter postures on the ground surface for diamond grinding are not enough. To enhance the practical usage of this processing technology, this work investigated the effects of cutter postures on the formed surface, and the formation mechanism of the machined surface and processing laws were analyzed. The logical architecture diagram of this paper is shown in Fig. 1. By coupling the multi-axis grinding, diamond grinding, and tool inclination angle effects, machining of complex parts made of hard and brittle materials could be achieved by this machining process. High-performance processing of hard and brittle materials can be innovatively achieved by a combination of these technical elements. Multi-view analysis of this kind of technology was conducted.

Taking advantage of this technology in vector-controllable and efficient processing of hard and brittle materials with

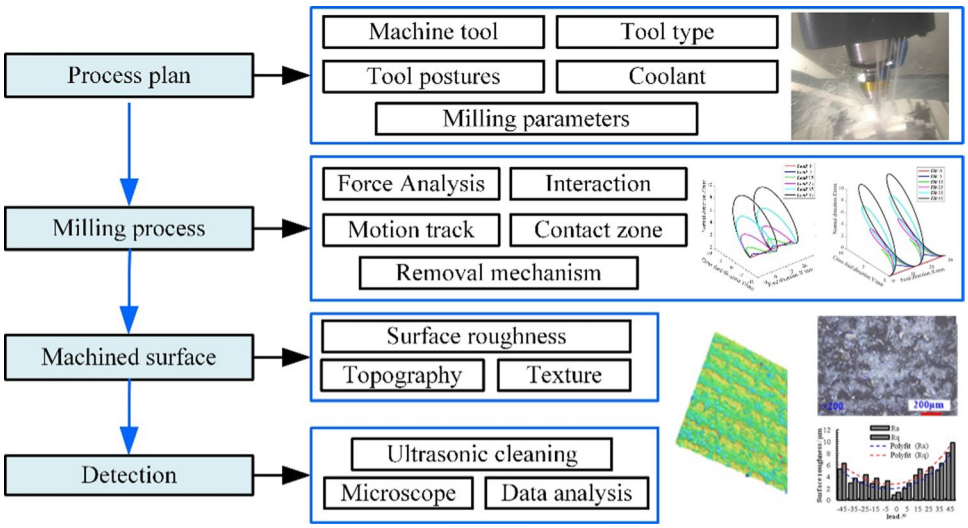


**Fig. 1** Logical architecture diagram of this work

complex features, combined with precision and ultra-precision processing technology, it can target high-performance advanced manufacturing of key functional components in the aerospace, medical engineering, optics, and semiconductor fields through coordinated control of quality, efficiency, and precision.

## 2 Experimental details

Firstly, the definition of tool inclination angles was analyzed. In general, the combination of single-tool inclination angles and grinding modes could be divided into eight types, and the schematic diagrams of each grinding condition are presented in Fig. 2.

In Fig. 2, different tool postures under conventional and down grinding processes are presented, and the arrow represents the approximate cutting space position and cutting characteristics of the engaged diamond abrasive particles. By analyzing the relative space positions between the engaged cutting parts of the diamond ball end grinding and the transition surface during the machining process, it is concluded that the effective cutting speed and movement space path are obviously different when adopting different grinding modes and tool inclination angles which even own the identical absolute value, and further material removal characteristics and surface formation condition would be significantly affected.

The experimental procedure is shown in Fig. 3. The multi-axis diamond grinding tests were conducted in a five-axis machine tool (Ultrasonic 80 eVo linear), the fixture uses the machine's four-jaw chuck, and the coolant is used in the grinding process. The ball end diamond cutters with a diameter of 10 mm and abrasive grain size about 140–150 microns are used, and the abrasive grain of the cutter is shown in Fig. 4. The quartz glass with dimensions of length 151 mm, width 36 mm, and height 26 mm was used in the practical machining, and the performance properties of quartz glass are presented in Table 1. The process parameters are presented in Table 2, and the fundamental process parameters are depth of cut ap 0.030 mm, width of cut ae 0.15 mm, spindle speed $n$ 6000 r/min, and feed speed $F$ 1200 mm/min. The cutting speed of the diamond grains corresponding to the maximum radius of the diamond tool could reach 188.4 m/min. The machined workpieces are cleaned with an ultrasonic cleaner and dried to be observed with a laser confocal microscope (KEYENCE VK-X200).

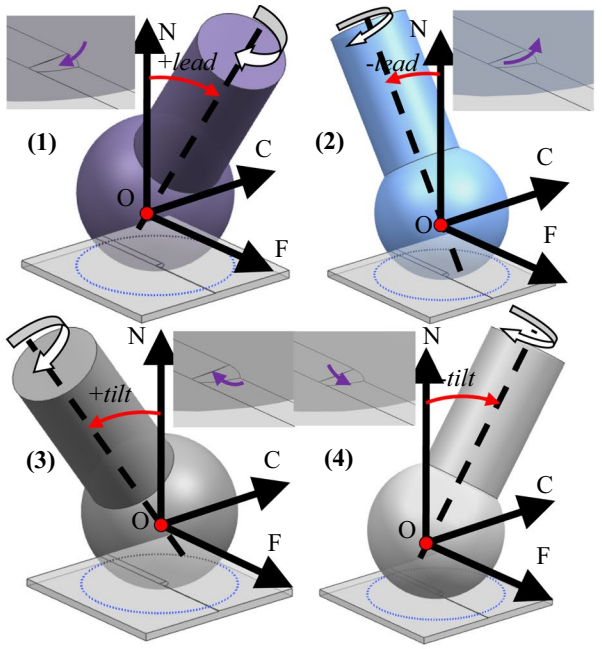


**(a)** Tool postures for conventional grinding

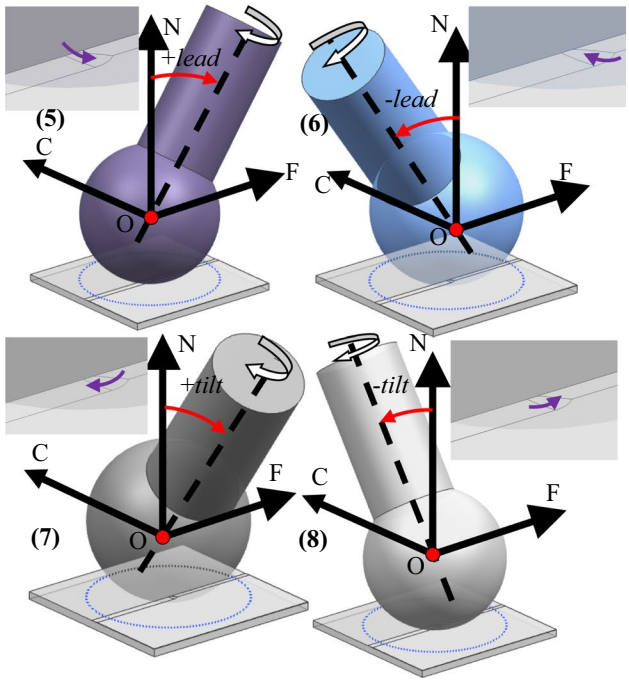


**(b)** Tool postures for down grinding

**Fig. 2** Tool postures and cutting characteristics

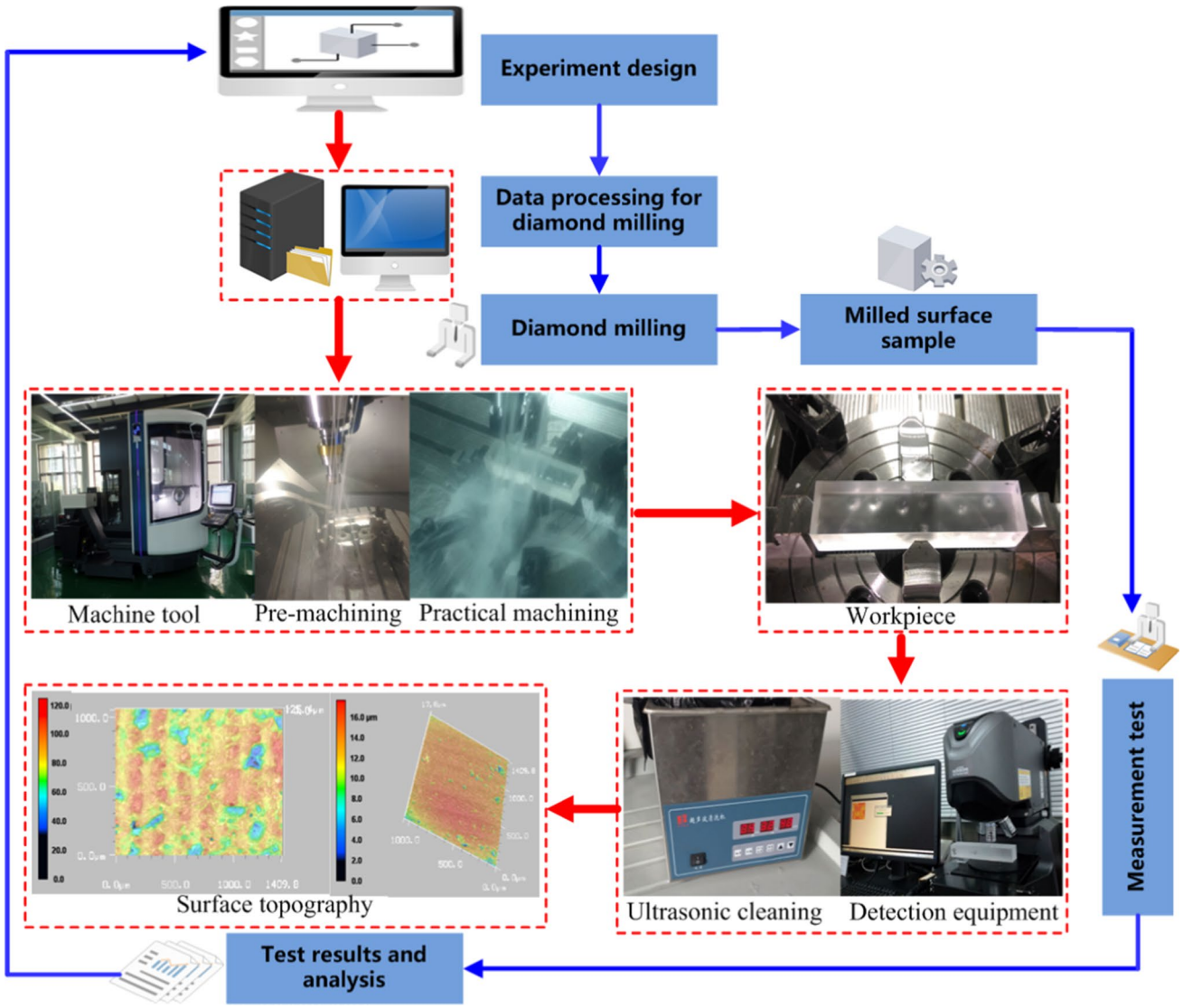


**Fig. 3** Flowchart of practical experiments

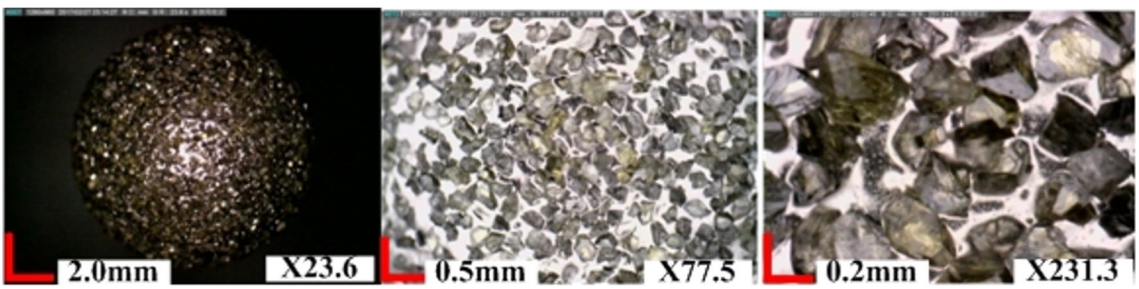


**Fig. 4** Abrasive grains on the cutter

**Table 1** Performance properties of quartz glass [4]

| Density | Young's modulus | Poisson's ratio | Torsional rigidity | Compression strength | Bending strength | Tensile strength | Vickers hardness |
|---|---|---|---|---|---|---|---|
| 2.2 g/cm$^3$ | 71.6 GPa | 0.17 | 31.4 | 1.1 GPa | 69 MPa | 55 MPa | 8.8–10.1 GPa |

**Table 2** Experimental parameters in the diamond milling process

| Experiment number | Variable | Value/° | | | | | | | | | | |
|---|---|---|---|---|---|---|---|---|---|---|---|---|
| No. 1 (conventional milling) | *Tilt* | −45 | −35 | −25 | −15 | −5 | 0 | 5 | 15 | 25 | 35 | 45 |
| No. 2 (conventional milling) | *Lead* | −45 | −35 | −25 | −15 | −5 | 0 | 5 | 15 | 25 | 35 | 45 |
| No. 3 (down milling) | *Tilt* | −45 | −35 | −25 | −15 | −5 | 0 | 5 | 15 | 25 | 35 | 45 |
| No. 4 (down milling) | *Lead* | −45 | −35 | −25 | −15 | −5 | 0 | 5 | 15 | 25 | 35 | 45 |

## 3 The spatial trajectory and characteristics of abrasive particles

### 3.1 Abrasive trajectory characteristics under different *lead* angles

The feed rate is represented by $F$ (mm/s), the tool radius is represented by $R$ (mm), the rotation speed is represented by $S$ ($n$/s), the *lead* angle is represented by *lead* (rad), the *tilt* angle is represented by *tilt* (rad), and the time is represented by $t$ (s).

When grinding with *lead* angle, the grain radius $r_G$ of abrasive point at the largest depth is defined by Eq. (1)

$$r_G = R \cdot \sin(lead). \tag{1}$$

Then, the abrasive trajectory in feed direction, cross-feed direction, and normal direction is calculated by Eq. (2):

$$\begin{cases} x = F \cdot t - \left(r_G - r_G \cdot \cos\left(2\pi \cdot S \cdot t\right)\right) \cdot \cos\left(lead\right) \\ y = r_G \cdot \sin\left(2\pi \cdot S \cdot t\right) \\ z = \left(r_G - r_G \cdot \cos\left(2\pi \cdot S \cdot t\right)\right) \cdot \sin\left(lead\right) \end{cases} \tag{2}$$

Under the condition of conventional grinding, the abrasive trajectory at the largest depth with different positive *lead* angles is presented in Fig. 5. When *lead* angle is 0, abrasive trajectory is a straight line. When there is a *lead* angle, the abrasive trajectory is an approximate spatial spiral, and the spiral diameter increases as the *lead* angle increases when the *lead* angle is less than 90°. The abrasive particles are cut in from the side of the feed direction, and the curvature of the cut increases as the *lead* angle increases.

The movement of the abrasive particles can be decomposed into feed motion and tangential motion. The force between the workpiece and the cutter can be divided into the squeezing force ($F_N$) generated by the abrasive feed motion and the tangential force ($F_T$) generated by the tangential motion. As shown in Fig. 6, when *lead* angle is 0, the abrasive grains at $P_1$ only have a feed speed, and the tangential speed is 0, and the material at this point is mainly subjected to normal extrusion. The line speed of the abrasive grain at $P_2$ is 20.62 mm/s, and the material at this point is simultaneously affected by the tangential force and the normal force. The tangential force direction is the same as the normal force direction when the abrasive particles are just cut in, and when the abrasive particles move to the position shown in the figure, the tangential force is perpendicular to the normal force. The final-formed surface of the workpiece is continuously processed by the abrasive particles at $P_1$.

However, when there is a lead angle, there is tangential velocity at $P_3$ and $P_4$. When the lead angle is 45°, the tangential velocity at $P_3$ is 133.29 mm/s, and that at $P_4$ is 147.07 mm/s, which is significantly higher than that without *lead* angle. As shown in Fig. 6c, a rectangular coordinate

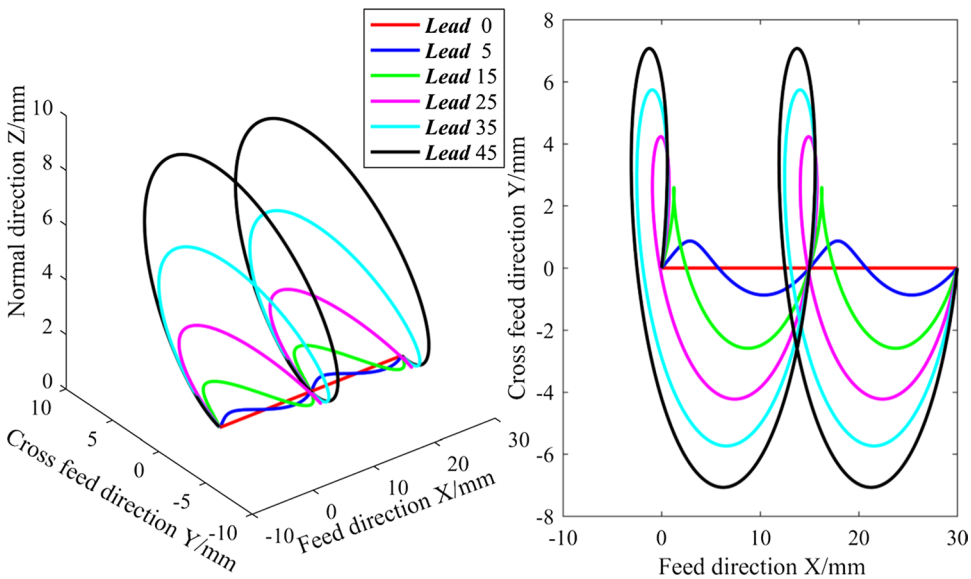


**Fig. 5** Abrasive trajectory at the largest depth with different *lead* angles

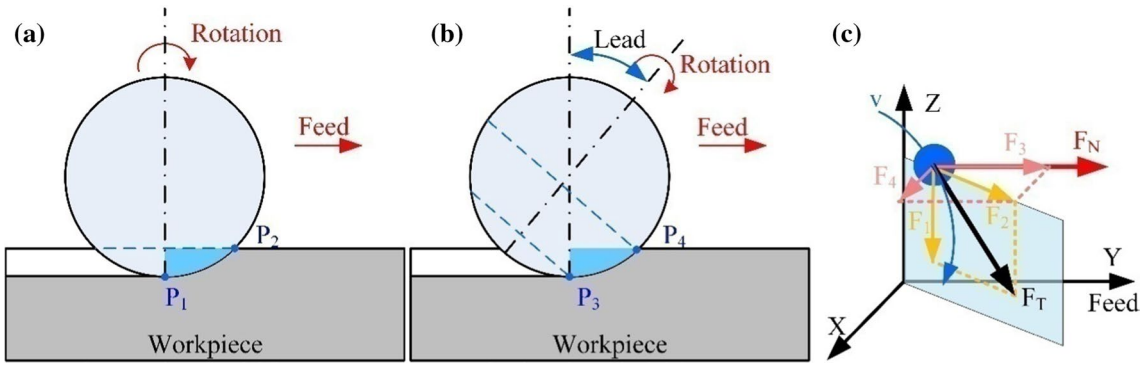


**Fig. 6** Interaction diagram, **a** without *lead*, **b** with *lead*

system is established with the feed direction as the *Y*-axis and the normal direction of the workpiece as the *Z*-axis. The abrasive particles are cut in at high speed from the side of the feed direction, and there is an angle (acute angle) between the tangential force and the normal force when the abrasive particles are just cut in, and $F_T$ is not on the YZ plane. $F_T$ can be decomposed into the forces $F_1$ and $F_2$ of a vertical extrusion workpiece, and $F_2$ can be decomposed into the forces $F_4$ parallel to the normal force and $F_3$ vertical to the normal force. With the movement of abrasive particles, $F_1$ and $F_3$ decreased and $F_4$ increased. The final-formed surface of the workpiece is formed by periodic grinding of the abrasive particles on the circumference at $P_3$.

## 3.2 Abrasive trajectory characteristics under *tilt* angles

When grinding with *tilt* angle, the grain radius $r_G$ of cut abrasive the largest depth is defined by Eq. (3)

$$r_G = R \cdot \sin(tilt) \tag{3}$$

Then, the abrasive trajectory in the feed direction, the cross-feed direction, and the normal direction is calculated by Eq. (4):

$$\begin{cases} x = F \cdot t + r_G \cdot \sin(2\pi \cdot S \cdot t) \\ y = \left(r_G - r_G \cdot \cos(2\pi \cdot S \cdot t)\right) \cdot \cos(tilt) \\ z = \left(r_G - r_G \cdot \cos(2\pi \cdot S \cdot t)\right) \cdot \sin(tilt) \end{cases} \tag{4}$$

Under the condition of conventional grinding, abrasive trajectory at the largest depth with different positive *tilt* angles is shown in Fig. 7. When *tilt* angle is 0, the track of the abrasive trajectory at the tool tip is a straight line, and the interaction between the abrasive particles and workpiece is continuous. When there is a *tilt* angle, the abrasive trajectory is a cycloidal line, and the abrasive particles are periodically contacted with the workpiece, and the swing amplitude increases as the roll angle increases. With the increasing *tilt*, the angle of abrasive cut-in decreases, and the proportion of contact time between single abrasive and workpiece in a single rotation cycle decreases.

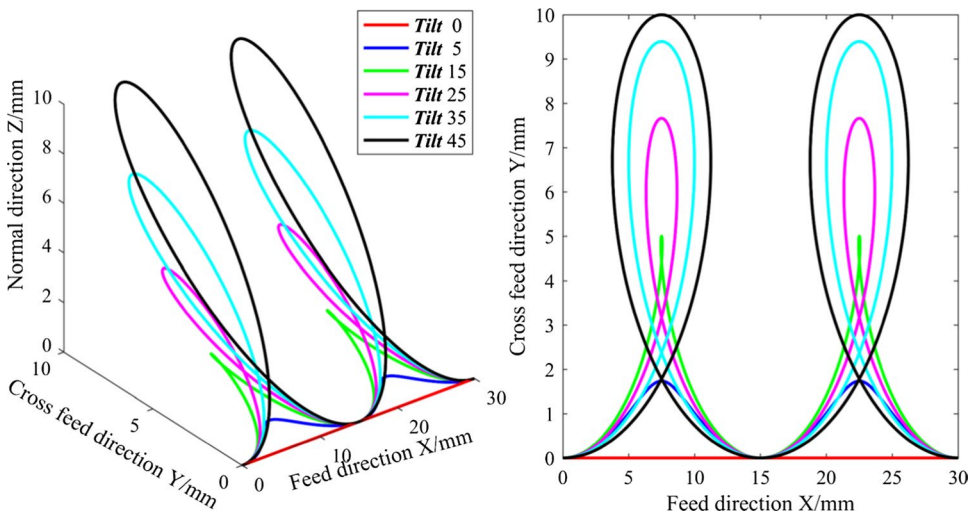


**Fig. 7** Abrasive trajectory at critical cutting point with different tilt angles

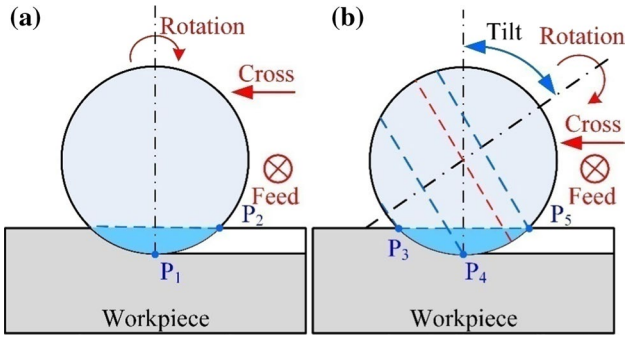


**Fig. 8** Interaction diagram, **a** without *tilt*, **b** with *tilt*

As shown in Fig. 8, when there is a *tilt* angle, the tangential velocity of abrasive particles on the contact arc line between the tool and workpiece is different, and the tangential velocity of abrasive particles at $P_3$, $P_4$ and $P_5$ increases in turn. Therefore, the workpiece materials at different spatial positions along the cross-feed direction will be affected by different forces, which will produce different processing effects. The removal of the abrasive particles at $P_4$ finally forms the machined surface, and the positive and negative of the same value of the *tilt* angle correspond to the different abrasive cutting speeds at $P_4$, thus affecting the final-formed surface characteristics. However, when there is no *tilt* angle, the extrusion action of abrasive particles exists in this place, and it is more conducive to forming a relatively flat surface (as shown in Figs. 8, 10).

## 4 Results and discussion

### 4.1 Machined surface topography

#### 4.1.1 Surface topographies under conventional grinding

A comparison of the machined surface topographies under *lead* angles is presented in Fig. 9, and effects of tool

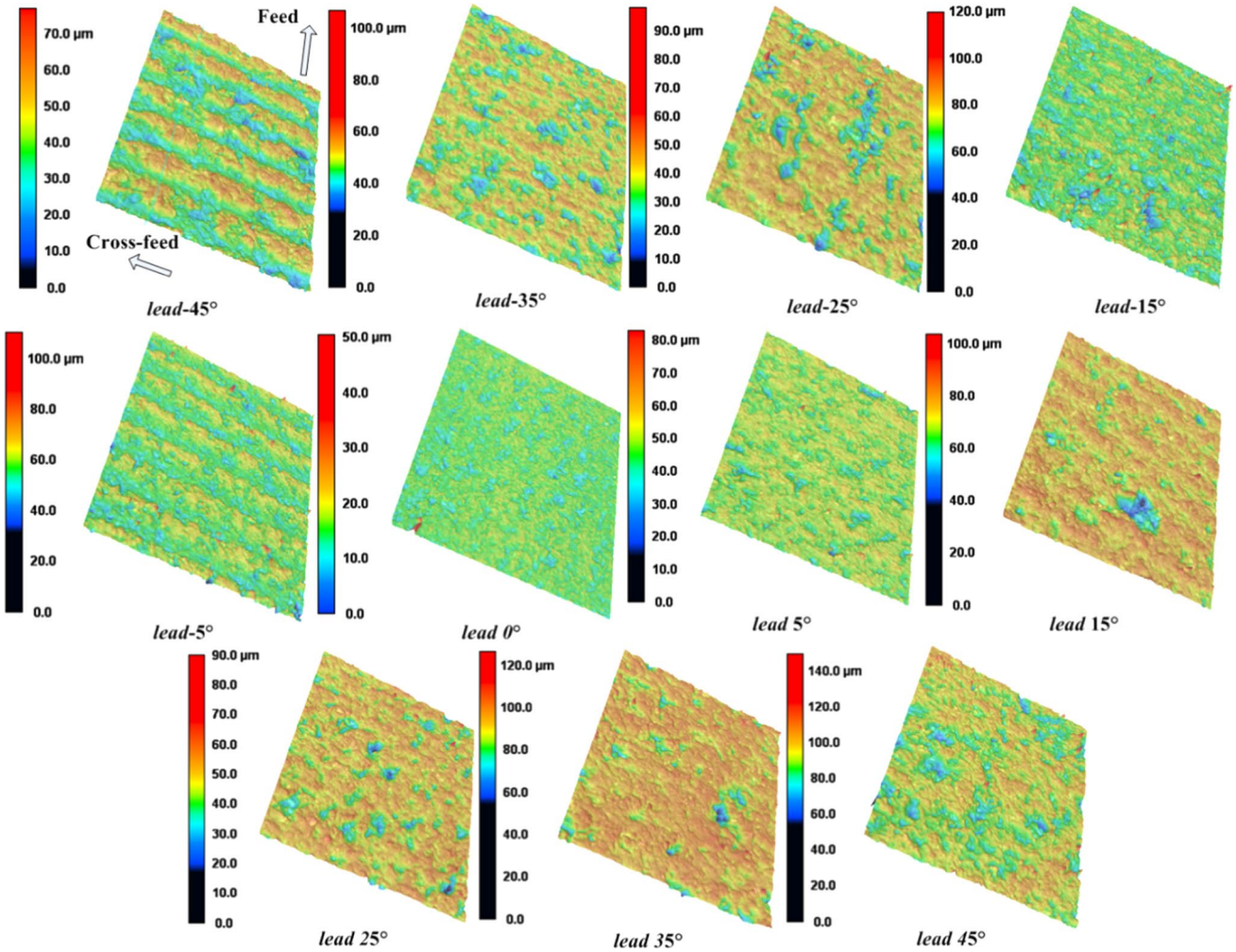


**Fig. 9** Surface topographies with regard to *lead* angles under conventional grinding

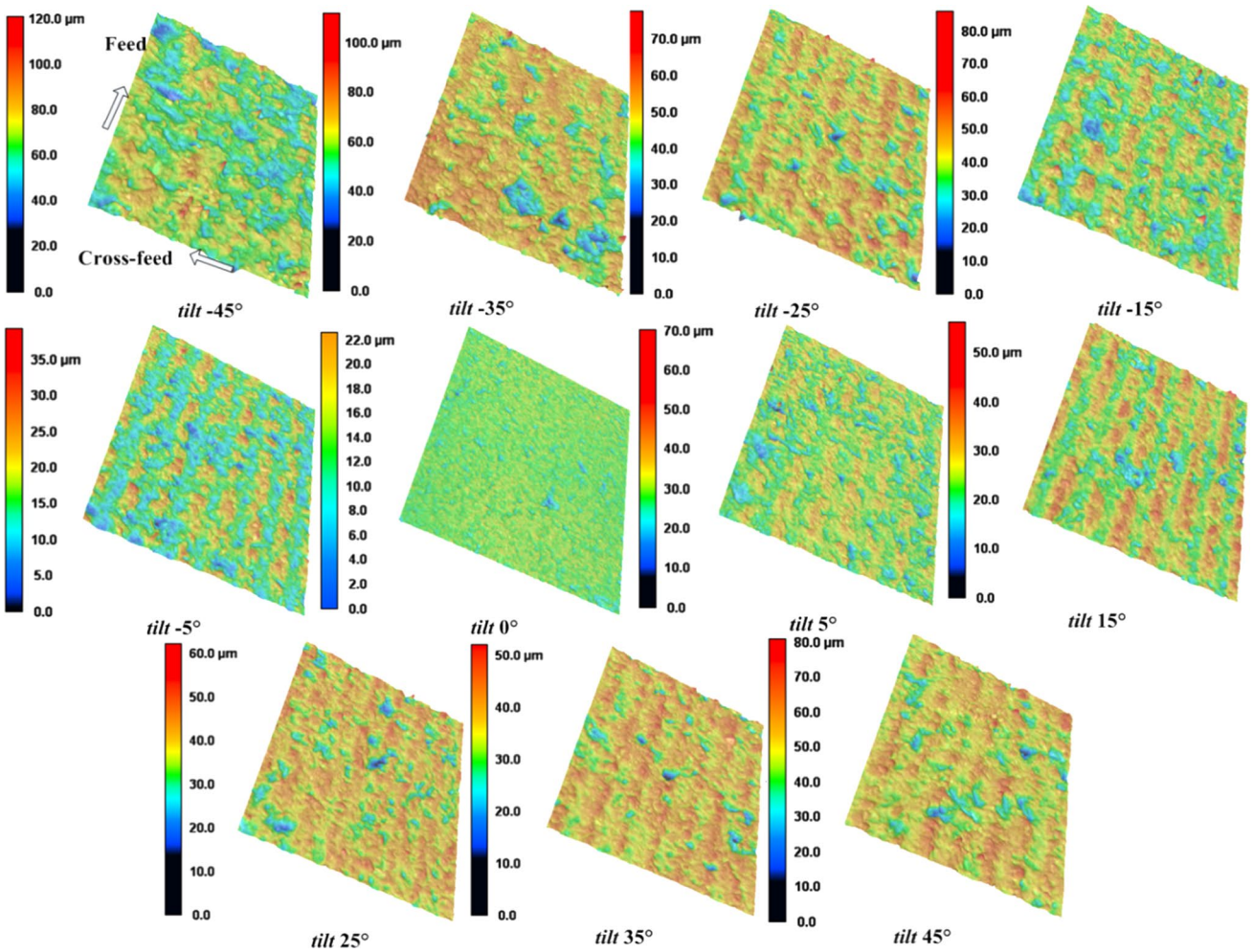


**Fig. 10** Surface topographies with regard to *tilt* angles under conventional grinding

postures on the corresponding roughness values are shown in Fig. 14a. Together with the analysis of cutting trajectory of the engaged abrasive particles shown in Fig. 1, it is found that structured textures for the ground surface under *lead* angles are parallel to cross-feed direction under conventional grinding, especially for negative *lead* angles, while roughness for ground surface with negative *lead* angles is smaller than positive *lead*. For negative *lead*, the engaged diamond abrasive particles are cut in near the final-formed surface and then cut out from the connection position between the uncut surface and the transition surface during the diamond grinding shown in Fig. 2a, which would induce extrusion action toward the final-formed surface to some extent. The undeformed chip thickness acts as a key factor that influences the machining effects in grinding process. During the initial cutting process deriving from movement of the engaged abrasives, the undeformed chip thickness changes from thin to thick, and the effective grinding speed of the engaged grains for positive *lead* is a bit larger than the one induced by negative *lead* with identical absolute value. However, the engaged abrasives are cut in near the top position of the transition surface and then cut out near the final-formed surface after interaction of friction with transition surface for positive *lead* presented in Fig. 2a. As interaction between the engaged grains and materials goes on, the undeformed chip thickness decreases to some extent.

In Fig. 10, textures of the ground surface are approximately parallel to feed direction, especially *tilt* −25°, *tilt* −15°, *tilt* −5°, and *tilt* 15°. While the concave and convex features are apparent under *tilt* −45°, *tilt* −35°, *tilt* 25°, and *tilt* 45°. In general, the undeformed chip thickness increases from small to large when negative *tilt* and negative *lead* were used, while the undeformed chip thickness decreases from large to small when employing positive *tilt* and positive *lead* for initial engagement stage under conventional grinding.

Machining modes are significantly influenced by the undeformed chip thickness (Liu et al. [8]). The material removal mode changes from plastic removal to brittle

fracture when the undeformed chip thickness increases to a specific value, and conversely the materials' brittle fracture would firstly happen during the material removal process. Inclination angles have a significant effect on the undeformed chip thickness, and further formation of the machined surface would be affected (Qiu et al. [13]).

When the diamond abrasives engaging with the workpiece materials, thermal expansion and mechanical pressure induced by the interaction behavior would produce stress inside the brittle material, and surface fractures happen when the materials stress exceeds the rupture strength [19]. Large-scale brittle fracture of material near the final-formed surface is not conducive to the formation of high-quality surface, and significant concave and convex features would be generated. The machined surfaces with significant surface fragmentation phenomena are mainly produced by materials' brittle fracture mode, such as positive *lead* angles with larger absolute value.

#### 4.1.2 Surface topographies under down grinding

Surface topographies produced by different tool postures are shown in Figs. 11 and 12 under down grinding condition. The texture of ground surface under *lead* − 5°, *tilt* − 25°, *tilt* − 15°, *tilt* 15°, and *tilt* 25° is structured, and the plastic removal state in diamond grinding of the quartz glass is reflected. The surface texture direction is mainly determined by feed direction of the cutter and initial cutting moment and geometry feature of the engaged diamond abrasives. Convex and concave features are significantly presented when adopting *lead* − 35°, *lead* − 25°, *lead* 25°, *tilt* − 35°, *tilt* 25°, *tilt* 35°, and *tilt* 45° under down grinding condition, and larger surface roughness corresponding to the above inclination angles is presented in Fig. 14b. The apparent brittle removal mode near the final-formed surface greatly influences formation of surface features. Ideal evenness of the ground surface could be obtained by using inclination angles about 0° for both *lead* and *tilt* angle under down grinding.

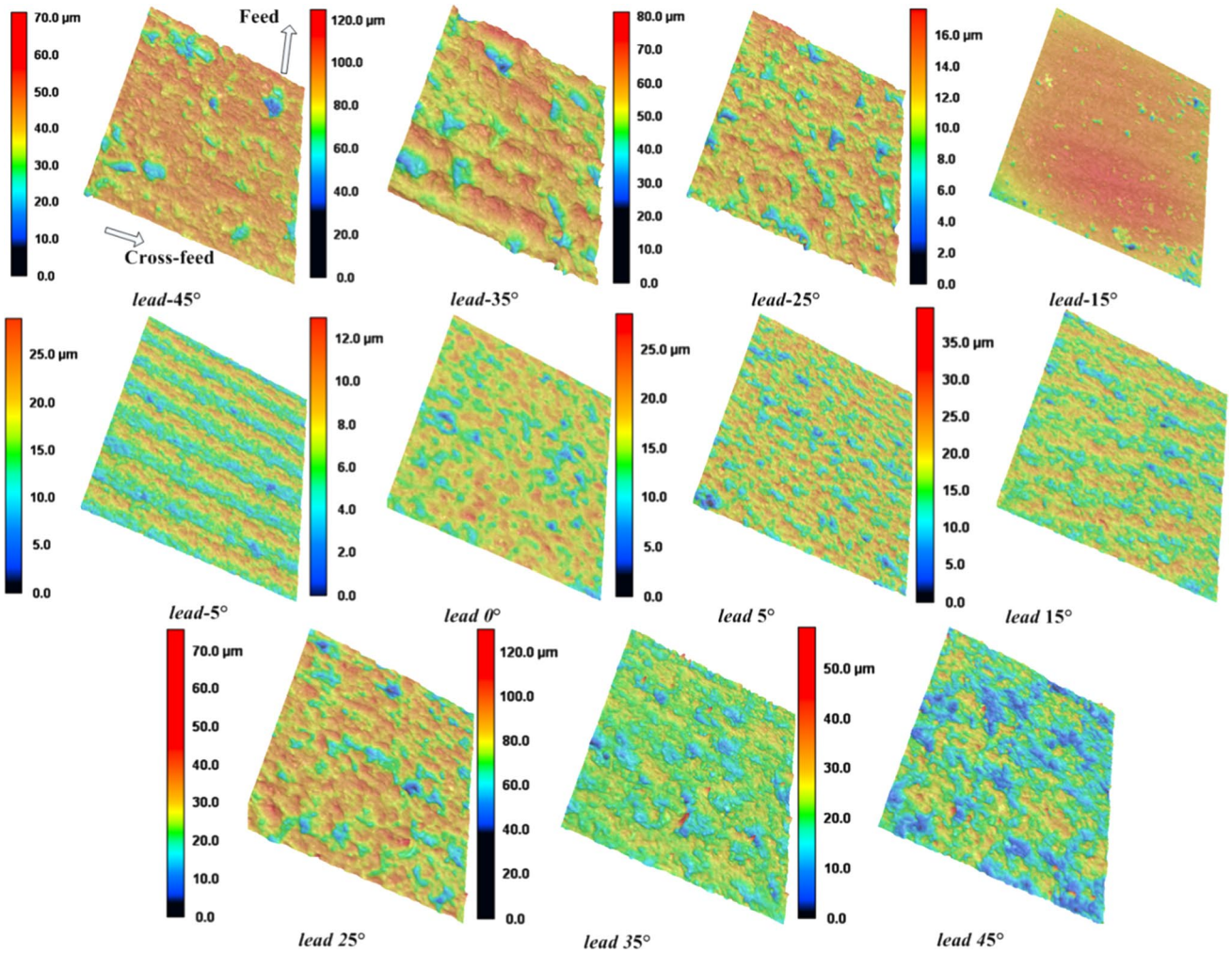


**Fig. 11** Surface topographies with regard to different *lead* angles (down grinding)

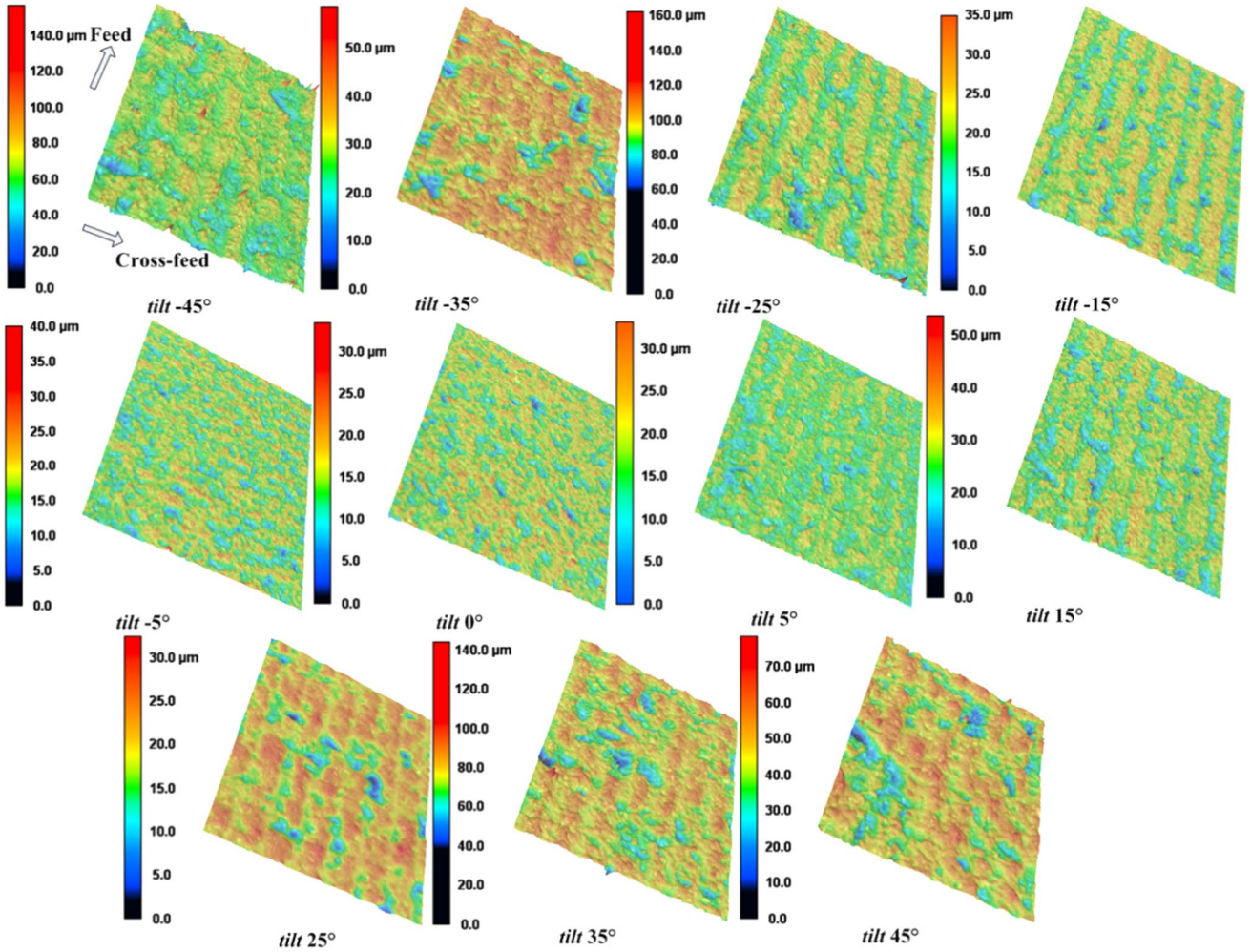


**Fig. 12** Surface topographies with regard to different *tilt* angles (down grinding)

Rotary extrusion effect of the engaged diamond abrasives toward the machined surface exists, and small-scale materials removal of brittle fracture together with plastic removal leads to significantly smaller concave and convex features on the final-formed surface.

When there is a *lead* angle, there is a periodic texture in the feed direction of the workpiece surface after machining, which is consistent with the motion characteristics of the abrasive particles periodically cutting in the feed direction (Fig. 5). When there is a *tilt* angle, the surface after processing has a periodic texture in the cross-feed direction, which is consistent with the characteristics of the different movement speeds of the abrasive grains in the cross-feed direction (Fig. 7).

## 4.2 Gray figures of the machined surface

Figure 13 shows the gray figures of the formed surface with larger surface roughness values, and the glass fragments with different colors under optical microscope could be significantly observed. The surface fragmentation phenomenon of the formed surface corresponding to larger roughness values is apparent. Compared with the surface topographies shown in Figs. 9, 10, 11, and 12, it could be found that the concave and convex features significantly appear in the final-formed surface.

## 4.3 Surface roughness

As *tilt* and *lead* increase, change laws of surface roughness are plotted in Fig. 14. The indicators Ra and Rp represent surface profile arithmetic average deviation and the mean square root value. The indicators Rz, Rp, and Rv represent the peak valley value, peak value, and valley value of the detection zone in the machined surface, respectively. Rz is equal to the sum of Rp and Rv. As the *lead* increases from −45° to 0°, surface roughnesses Ra and Rq decrease. When *lead* increases from 0° to 45°, Ra and Rq apparently

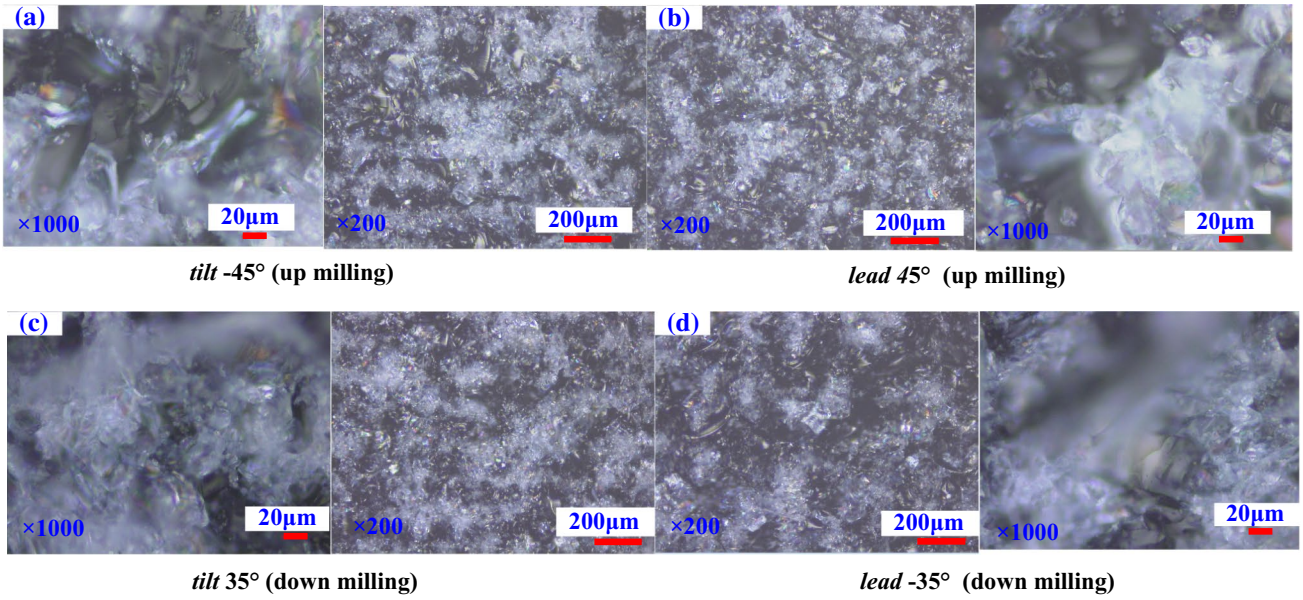


**Fig. 13** Surface fragmentation with larger surface roughness under conventional and down grinding

increase for conventional grinding. It could be found that more rough surface with larger roughness values could be produced under positive *lead* than negative *lead* with identical absolute values, which is significantly affected by the engagement action between the abrasive grains and workpiece materials for specific tool posture. Compared with the peak valley value corresponding to the other tool postures under conventional grinding conditions, the machined surface peak valley values generated by employing negative *lead* are relatively smaller, which is beneficial to manufacture the ground surface with high smoothness.

Variations in Ra, Rq, Rz, Rp, and Rv present the overall trend of bimodal shape when *lead* angle increases from −45° to 45° for down grinding condition, as plotted in Fig. 14b. In general, adopting positive *lead* could generate smaller surface roughness than negative *lead* and minimum surface roughness could be obtained when using *lead* angles nearby 0°.

As a whole, the similar variation trend of surface roughness Ra and Rq is presented as *tilt* angle increases for both conventional and down grinding, as shown in Fig. 14. Minimum roughness Ra and Rq could be generated by adopting *tilt* 0° for conventional grinding and *tilt* 5° for down grinding. In general, the ground surface with smaller roughness could be obtained by employing positive *tilt* than negative *tilt* under conventional grinding, while adopting negative *tilt* is beneficial to achieve smaller roughness values than positive *tilt* with the same value for down grinding. Variations trend of Rz, Rp, and Rv is approximately identical to each other. The interaction angle between the approximate axis of the abrasive space moment trajectory and normal direction of the machining area is relatively larger when adopting relatively larger *tilt* or *lead* angles, and then the direction and value of the cutting speed of engaged abrasives would be significantly affected. Finally, the undeformed chip thickness of materials removal varies with the variations in inclination angles, which would directly affect the materials removal modes and surface roughness.

In general, employing *lead* angles could provide relatively smaller surface peak valley Rz values than using *tilt* angles for conventional grinding, while adopting *tilt* angles is beneficial to achieve smaller peak valley values comparing with usage of *lead* angles under down grinding. Further, peak valley values under conventional grinding are larger than peak valley values corresponding to down grinding when adopting *tilt* angles, while peak valley values under conventional grinding are significantly smaller than peak valley values under down grinding when *lead* angles are adopted, especially when using negative *lead* (Fig. 14).

Employing negative *lead* or positive *tilt* for conventional grinding and positive *lead* or negative *tilt* for down grinding tends to produce smaller surface roughness, and the corresponding machining postures are presented in Figs. 2 (2), (3), (5), and (8), respectively. When adopting negative *lead* for conventional grinding and positive *lead* for down grinding, the diamond abrasives are cut in at the position nearby final-formed surface and then cut out at the uncut surface. However, the diamond abrasives are approximately cut in at the surface locations produced by the adjacent cutting path and then cut out at the surface produced by the current cutting path when adopting positive *tilt* under conventional grinding. When applying negative *tilt* under down grinding,

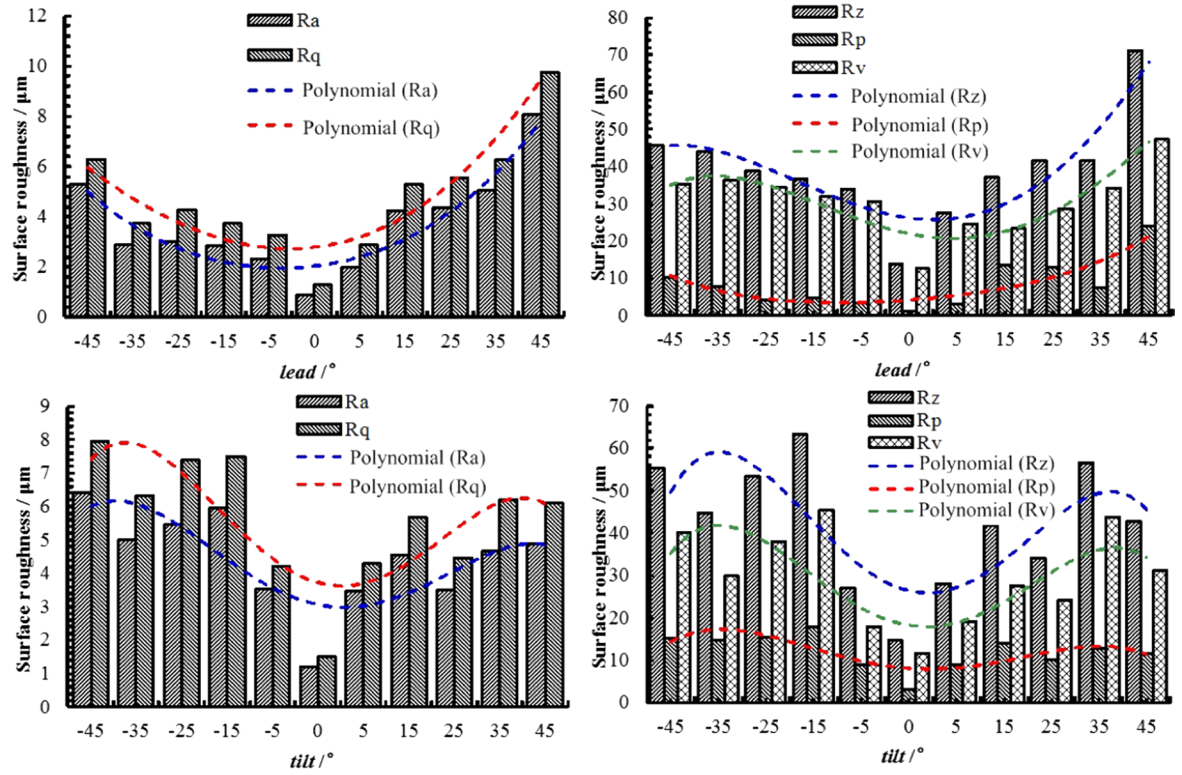


**(a)** Variations of Ra, Rq, Rz, Rp, and Rv (conventional grinding)

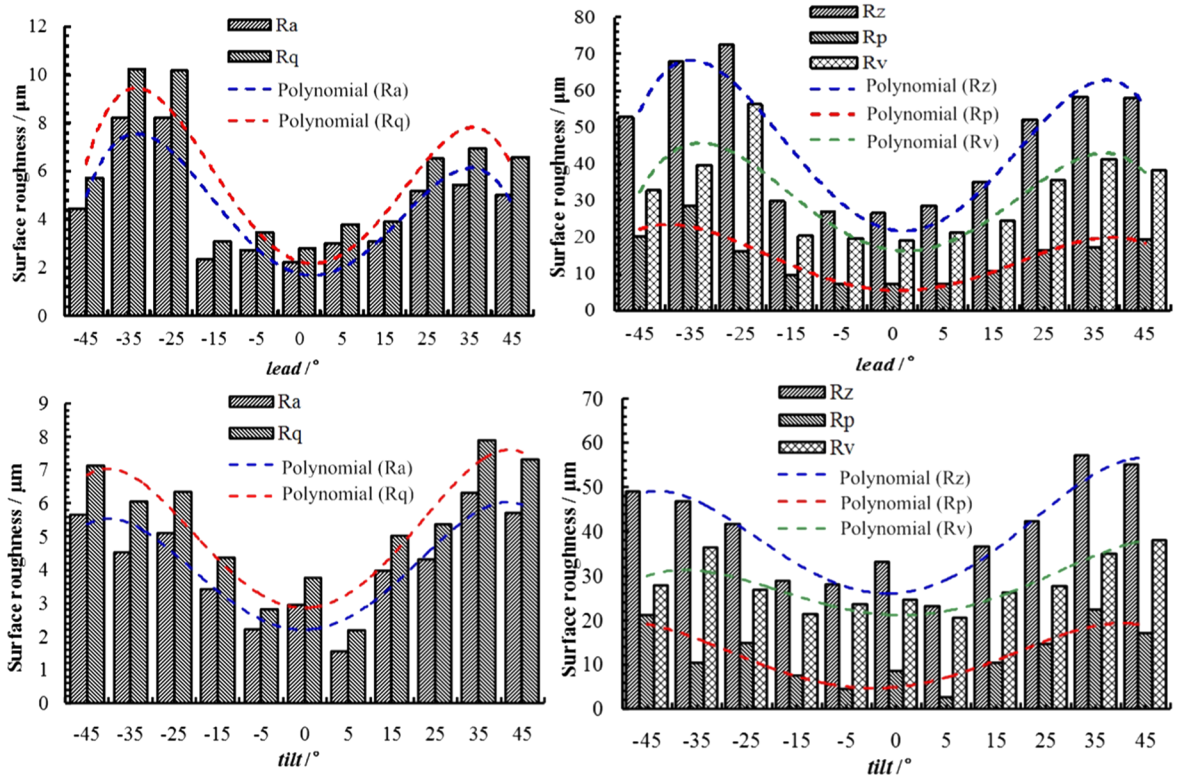


**(b)** Variations of Ra, Rq, Rz, Rp, and Rv (down grinding)

**Fig. 14** Surface roughness with inclination angles under conventional and down grinding

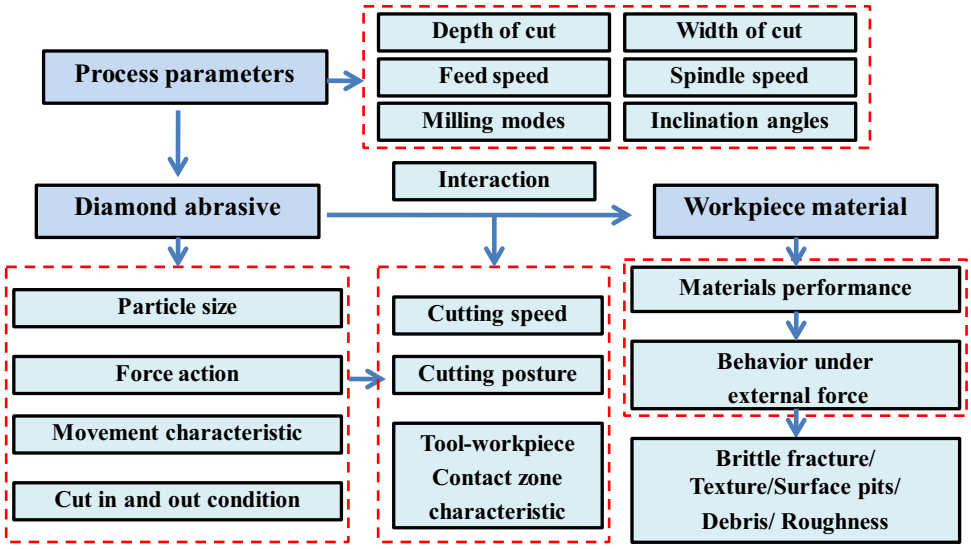


**(a)** Relationship among the various factors induced in the diamond grinding process

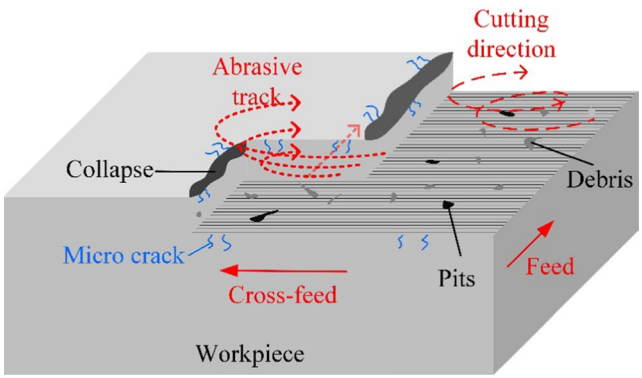


**(b)** Surface formation phenomena

**Fig. 15** Schematic diagram of diamond abrasive grain processing and surface forming

the diamond abrasives are cut in at the surface produced by the current cutting path and then cut out at the surface produced by the adjacent cutting path. The cutting trajectory and cutting characteristics of the above process condition corresponding to smaller surface roughness are beneficial to make the crack initiation extension location away from the final-formed surface, and negative effect of brittle fracture during the material removal process on the final-formed surface could be mitigated.

### 4.4 Analysis of diamond abrasive processing and surface forming

The schematic diagram of diamond abrasive grain processing and surface formation is presented in Fig. 15. When grinding hard and brittle quartz glass with diamond ball end cutters, the processing parameters, inclination angle, and grinding mode determine the characteristics of the action area between diamond abrasive grains and workpiece materials (Fig. 2). The grain size, motion characteristics (Figs. 5, 7), cutting characteristics, and force of diamond abrasive grains with high frequency act on the material to be removed through cutting speed and cutting attitude in the tool–work interaction region. Inherent properties of the material are subjected to dynamic loading, and after the yield strength of the material is reached, microcrack initiation and expansion occur, and brittle fracture depending on the dip effect occurs further. Then, small-scale block brittle removal is generated, and the removed material is peeled off from the substrate to generate debris; at the same time, brittle fracture occurs inside the surface material, and microscale pit features remain on the partially processed surface (Figs. 9, 10, 11, 12, 13); the direction of abrasive cutting speed of the near-formed surface determines the surface texture orientation; the various geometric, moving, physical and other factors in the entire processing system combine to form a hard and brittle material forming surface.

## 5 Conclusions

In this work, the grinding of quartz glass at different angles of the ball end diamond grinding cutter was studied. Firstly, through the kinematics modeling analysis, the characteristics of the trajectory of the abrasive particles and the form of the force are analyzed. Then, the processing surface was tested and analyzed, and the material removal characteristics and surface forming rules of the variable-axis processing quartz glass were summarized. The main conclusions are as follows:

1. According to the abrasive kinematic characteristics, when the tool uses *lead* angle, the abrasive particles are periodically cut from the side of feed direction, and the greater the *lead*, the greater the cutting speed of the abrasive. During the movement of the abrasive, the direction of the force with the workpiece changes continuously. This is consistent with the feature that the formed surface has a periodic texture along the feed direction; when there is a roll angle, the periodic plunging of the abrasive grains from the feed direction, the angle, and speed of the cut are increased with the *tilt* angle increase. The tangential velocity of the different contact points of the abrasive grains and the workpiece in the transverse feed direction is different, and the force will also be different, which is consistent with the feature that the formed surface has a periodic texture along the cross-feed direction.
2. Material removal characteristics and surface formation conditions would be significantly affected by the effective cutting speed and movement space path derived from different grinding modes and tool inclination angles which even own the identical absolute value. Also, change in the undeformed chip thickness in the initial engagement process differs under various inclination angles. The surface textures are approximately determined by feed direction and space cutting trajectory of engaged abrasives, while the concave and convex features are apparent under *tilt* $-45°$, *tilt* $-35°$, *tilt* $25°$, and *tilt* $45°$.
3. The significant concave and convex features and surface fragmentation phenomenon would be generated when large-scale brittle fracture of workpiece material near the final-formed surface happens, such as larger positive *lead* or smaller negative *tilt* under conventional grinding and smaller negative *lead* or larger positive *tilt* under down grinding. Apparent surface fragmentation phenomenon appears when the corresponding surface roughness values are large.
4. Ideal surface evenness could be obtained by using inclination angles about $0°$ for both *lead* and *tilt* angles under conventional or down grinding conditions. Rotary extrusion effect of the engaged diamond abrasives toward the machined surface exists, and small-scale materials removal of brittle fracture together with plastic removal would lead to less geometrical features of concave and convex characteristic on the ground surface.
5. As *lead* increases from $-45°$ to $45°$, surface roughness Ra and Rq decreases at the initial stage and then increases for conventional grinding. On the whole, the ground surface with smaller roughness could be produced by employing negative *lead* than positive *lead* with the same values. Variations in surface roughness present the overall trend of bimodal shape when *lead* angle increases from small to large under down grinding conditions. As *tilt* angle increases in the designed range, surface roughnesses Ra and Rq slightly increase at the initial stage and then apparently decrease with the following increment for conventional and down grinding. Minimum surface roughness appears under inclination angles about $0°$ for conventional grinding and down grinding. Smaller surface roughness could be generated by employing negative *lead* or positive *tilt* for conventional grinding and positive *lead* or negative *tilt* for down grinding condition with the cutting trajectory and cutting characteristics that are beneficial to make the crack initiation extension location away from the final-formed surface.

**Acknowledgements** This work is funded by the National Natural Science Foundation of China (51505468), the ninth special funding of China Postdoctoral Science Foundation Project (2016T90555), and the China Postdoctoral Science Foundation (2015M571907).

## References

1. Matsumura T, Aristimuno P, Gandarias E, Arrazola PJ (2013) Cutting process in glass peripheral milling. J Mater Process Technol 213(9):1523–1531
2. Pawar P, Ballav R, Kumar A (2017) Micromachining of borosilicate glass: a state of art review. Mater Today Proc 4(2):2813–2821
3. Zhang C, Rentsch R, Brinksmeier E (2005) Advances in micro ultrasonic assisted lapping of microstructures in hard–brittle materials: a brief review and outlook. Int J Mach Tools Manuf 45(7–8):881–890
4. Chen S-T, Jiang Z-H (2015) A force controlled grinding-milling technique for quartz-glass micromachining. J Mater Process Technol 216:206–215
5. Tuysuz O, Altintas Y, Feng H-Y (2013) Prediction of cutting forces in three and five-axis ball-end milling with tool indentation effect. Int J Mach Tools Manuf 66:66–81
6. Singh RP, Singhal S (2016) Rotary ultrasonic machining: a review. Mater Manuf Processes 2016(31):1795–1824
7. Karpat Y (2009) Investigation of the effect of cutting tool edge radius on material separation due to ductile fracture in machining. Int J Mech Sci 51(7):541–546

8. Liu K, Li XP, Liang SY, Liu XDE (2004) Society of manufacturing, nanometer scale ductile mode cutting of soda-lime glass. Society for Manufacturing Engineers, Dearborn
9. Arif M, Rahman M, San WY (2012) Analytical model to determine the critical conditions for the modes of material removal in the milling process of brittle material. J Mater Process Technol 212(9):1925–1933
10. Shao Y, Li B, Liang SY (2015) Predictive modeling of surface roughness in grinding of ceramics. Mach Sci Technol 19(2):325–338
11. Perveen A, Jahan MP, Rahman M, Wong YS (2012) A study on microgrinding of brittle and difficult-to-cut glasses using on-machine fabricated poly crystalline diamond (PCD) tool. J Mater Process Technol 212(3):580–593
12. Yao Z, Gu W, Li K (2012) Relationship between surface roughness and subsurface crack depth during grinding of optical glass BK7. J Mater Process Technol 212(4):969–976
13. Qiu Y, Gu ML, Zhang FG, Wei Z (2014) Influence of tool inclination on micro-ball-end milling of quartz glass. Mater Manuf Process 29(11–12):1436–1440
14. Ab Karim MS, Aly Diaa Mohammed Sarhan A, Hamdi Abd Shukor M (2011) Experimental study on minimizing edge chipping in glass milling operation using an internal CBN grinding tool. Mater Manuf Process 26(8):969–976
15. Arif M, Rahman M, San WY (2012) An experimental investigation into micro ball end-milling of silicon. J Manuf Process 14(1):52–61
16. Foy K, Wei Z, Matsumura T, Huang Y (2009) Effect of tilt angle on cutting regime transition in glass micromilling. Int J Mach Tools Manuf 49(3–4):315–324
17. Guo XG, Zhai RF, Kang RK, Jin ZJ, Guo DM (2019) Study of the influence of tool rake angle in ductile machining of optical quartz glass. Int J Adv Manuf Technol 104(1–4):803–813
18. Chen XX, Zhao J, Zhang WW (2015) Influence of milling modes and tool postures on the milled surface for multi-axis finish ball-end milling. Int J Adv Manuf Technol 77(9–12):2035–2050
19. Ding A, Wu Y, Liu Y (2011) Surface topography of fine-grained ZrO2 ceramic by two-dimensional ultrasonic vibration grinding. J Wuhan Univ Technol-Mater Sci Ed 26(6):1162–1165

**Publisher's Note** Springer Nature remains neutral with regard to jurisdictional claims in published maps and institutional affiliations.